Structures, Dynamics, and Reactivity of Tripodal Amido Ligands Coordinated to Ti^{IV} Centres

Stefan Friedrich[a], **Lutz H. Gade***[a], **Andrew J. Edwards**[b], and **Mary McPartlin**[b]

Institut für Anorganische Chemie der Universität Würzburg[a],
Am Hubland, D-97074 Würzburg, F.R.G.

School of Chemistry, The University of North London[b],
Holloway Rd, London N7 8DB, U.K.

Received April 14, 1993

Key Words: Titanium amido complexes / Tripodal ligands / Ligand dynamics / μ_2-Imido complex

A new class of amido titanium(IV) halides containing tripodal ligands $H_3CC(CH_2NR)_3TiX$ (R = Me, X = Cl: **1**; R = Me_3Si, X = Cl: **2a**, Br: **2b**; R = $SiMe_2tBu$, X = Cl: **3a**, Br: **3b**) has been synthesised. Compound **1** has been structurally characterised by X-ray crystallography and found to be dimeric in the crystal displaying an idealised C_2 symmetry with bridging amido functions linking the two halves of the molecule. The dimeric structure is retained in solution as has been shown by ^1H- and ^{13}C-NMR spectroscopy which has also revealed a high degree of ligand dynamics, effecting the interconversion of the two enantiomeric forms of the molecule. This process has been investigated by variable temperature NMR studies and phase-sensitive ^1H-NOESY/EXSY spectra. The dimeric μ-imido complexes $[H_3CC(CH_2NSiMe_3)_2(H)CH_2NTiX]_2$ (X = Cl: **4a**, Br: **4b**) have been isolated as a byproduct in the synthesis of **2a/b**, and a single-crystal X-ray structure analysis of **4a** has established its molecular structure.

Polydentate alkyl- or silylamides combine a number of virtues which make them ideal ligand systems for early transition metals in high oxidation states[1]. They offer a set of donor atoms which meets the electronic requirements of highly Lewis acidic metal centres and an efficient kinetic stabilisation of these complexes by steric shielding of a large sector of their coordination sphere. The possibility of designing a remaining reactive site of variable size and geometry at which metal-mediated transformations may take place provides an additional stimulus for their application.

These conceptual considerations have recently found their most prominent manifestation in the synthesis of a number of novel transition azametallatranes (**A**) along with the study of their structural chemistry as well as chemical and redoxchemical reactivity[2–6].

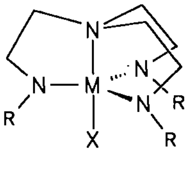

A

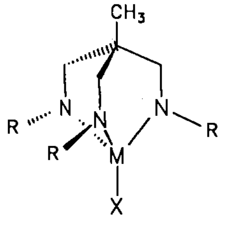

B

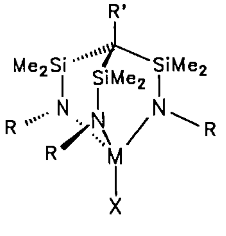

C

By introducing bulky silyl groups in **A** (e.g. R = tBu-$SiMe_2$) it has been possible to stabilise and characterise trigonal-monopyramidal M^{III} complexes of the early and middle first row transition metals, a coordination geometry which is rarely observed within ligand shells comprising monodentate ligands[6]. This shielding of the remaining reactive site in what would otherwise be a trigonal-bipyramidal complex marks the one extreme in the exploitation of the steric properties of such ligand systems. Our aim of employing transition metal amido complexes as building blocks in the synthesis of more complex structural arrays necessitated the design of chelating amides which leave a larger coordination arc at the metal centre than that available in structures of type **A** while offering the kinetic and thermodynamic stability of a chelating ligand. To this end we synthesised a series of trifunctional amines which may be employed as precursors in the preparation of compounds of type **B** and **C**. The structural characterisation of their trilithiated derivatives both in solution and in the solid state has already been published[7,8]. In this paper we report the synthesis, structures, and studies of the dynamic properties in solution of titanium amides of the general type **B**.

Results and Discussion

A. Reactions of $[H_3CC\{CH_2N(Li)R\}_3]_2$ (R = Me, $SiMe_3$, $SiMe_2tBu$) with $TiX_4(THF)_2$ (X = Cl, Br)

The reactions of the in situ generated lithium amides $[H_3CC\{CH_2N(Li)R\}_3]_2$ (R = Me, $SiMe_3$, $SiMe_2tBu$) with $TiX_4(THF)_2$ (X = Cl, Br) in pentane or pentane/diethyl ether (2:1) afford the corresponding amidotitanium complexes $[H_3CC(CH_2NR)_3TiX]_x$ in moderate yields (Scheme 1). The silyl-substituted tripodal amides are moderately moisture-sensitive orange oils which may be isolated and purified by vacuum distillation and are completely miscible with hydrocarbon solvents. The ^1H-, ^{13}C-, and ^{29}Si-NMR spectra are indicative of an overall threefold molecular symmetry as postulated above for the type **B** amido complexes.

Chem. Ber. **1993**, *126*, 1797–1805 © VCH Verlagsgesellschaft mbH, D-69451 Weinheim, 1993 0009–2940/93/0808–1797 \$ 10.00+.25/0

The product of the reaction of $[H_3CC\{CH_2N(Li)Me\}_3]_2$ with $TiCl_4(THF)_2$ crystallised from the toluene extract of the reaction mixture and was isolated as a highly moisture-sensitive deep red solid the analytical data of which were consistent with its formulation as $H_3C(CH_2NMe)_3TiCl$ (**1**). However, its relatively low solubility in aliphatic as well as aromatic hydrocarbon solvents and the complicated resonance patterns in the NMR spectra (vide infra) indicated an oligomeric, most probably dimeric, stucture. A conceivable dimerisation through Cl bridges similar to the situation found in polymeric $[Me_2NTiCl_3]_n$, thus generating a structural arrangement with an overall C_s symmetry, was inconsistent with the apparent absence of any molecular symmetry in the low-temperature limit spectra. Since the detailed geometry of the alternative dimerisation through a Ti−N edge could not be deduced from the spectral data, the stucture of **1** was determined by X-ray crystallography.

Scheme 1. The synthesis of **1**−**3**; i: $+[H_3CC\{CH_2N(Li)CH_3\}_3]_2$ in diethyl ether/pentane (1:2); ii: $+[H_3CC\{CH_2N(Li)\text{-}SiMe_2R\}_3]_2$ (R = Me, *t*Bu) in pentane

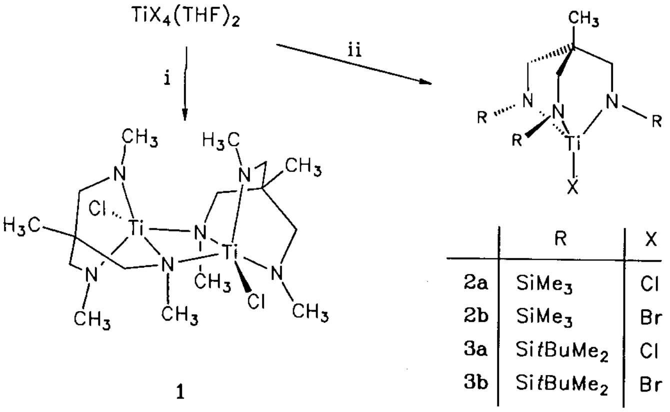

	R	X
2a	SiMe₃	Cl
2b	SiMe₃	Br
3a	Si*t*BuMe₂	Cl
3b	Si*t*BuMe₂	Br

B. X-ray Structure Analysis of $[H_3CC(CH_2NMe)_3TiCl]_2$ (1)

A single-crystal X-ray structure analysis of **1** established its dimeric structure as shown in Figure 1 along with the principal bond distances and interbond angles.

The dimer has idealised C_2 symmetry, the two halves of the molecule being related to each other by a twofold axis orthogonal to the Ti−Ti vector. Neither the formal oxidation state of the two five-coordinate metal centres nor their interatomic distance [*d*(Ti−Ti) = 3.142(3) Å] indicates any direct interaction between them. The Ti−N distances of the non-bridging amido functions lie in the range of 1.839(9)−1.879(9) Å and are thus comparable to those found in mono-[9] as well as dialkylamides such as $(Me_2N)_3TiCl$ [*d*(Ti−N) = 1.866(4) Å][10], $(Et_2N)_3TiCl$ (1.861 Å)[10], $(Me_2N)_2Ti[OC_6H_2(tBu)_3]_2$ [1.878(5) Å][11], and $(Me_2N)_2Ti(O_2CNMe_2)_2$ [1.882(5) Å][12] but are somewhat shorter that those observed in various chelating and non-chelating silylamides [*d*(Ti−N) > 1.90 Å][12−15]. The nitrogen atoms N(b), N(c), N(e), N(f) have an almost planar geometry, as has been found in virtually all structurally characterised transition metal amido complexes.

The bridging amido functions display an interesting bond length pattern depicted in Figure 2.

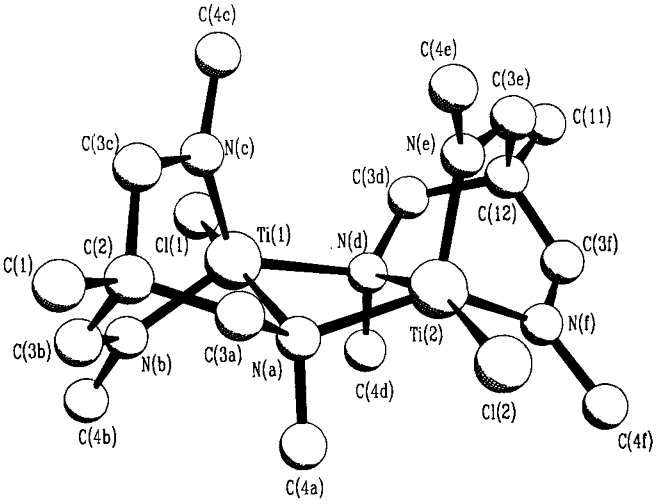

Figure 1. Molecular structure of **1** in the crystal as determined by an X-ray crystal structure analysis. Selected bond lengths [Å] and interbond angles [°]: Ti(1)−Ti(2) 3.142(3), Ti(2)−N(d) 2.140(9), Ti(1)−N(a) 2.153(9), Ti(2)−N(e) 1.839(9), Ti(1)−N(b) 1.879(9), Ti(2)−N(f) 1.863(10), Ti(1)−N(c) 1.844(10), Ti(1)−Cl(1) 2.351(4), Ti(1)−N(d) 2.034(9), Ti(2)−Cl(2) 2.354(4), Ti(2)−N(a) 2.073(8); N(a)−Ti(1)−N(d) 78.4(3), C(4c)−N(c)−Ti(1) 127.1(9), N(a)−Ti(2)−N(d) 78.9(3), C(4b)−N(b)−Ti(1) 130.4(8), Ti(1)−N(a)−Ti(2) 96.0(4), C(4c)−N(c)−C(3c) 115(1), Ti(1)−N(d)−Ti(2) 96.1(4), C(4b)−N(b)−C(3b) 113.4(9), N(a)−Ti(1)−Cl(1) 162.9(3), C(4a)−N(a)−C(3a) 110.3(9), N(d)−Ti(2)−Cl(2) 161.2(3), C(4a)−N(a)−Ti(1) 115.1(7), C(4f)−N(f)−Ti(2) 133.1(8), C(4a)−N(a)−Ti(2) 104.5(7), C(4e)−N(e)−Ti(2) 127.2(8), C(4d)−N(d)−C(3d) 109.9(9), C(4f)−N(f)−C(3f) 111(1), C(4d)−N(d)−Ti(2) 116.5(7), C(4e)−N(e)−C(3e) 116.2(9), C(4d)−N(d)−Ti(1) 105.2(6)

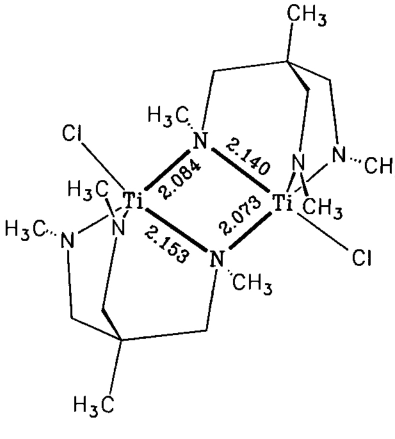

Figure 2. Ti−N bond length pattern within the central Ti_2N_2 unit of **1**

The Ti−N bonds which connect the two halves of the molecule [Ti(1)−N(d), Ti(2)−N(a)] are considerably shorter [*d*(Ti−N) = 2.078 Å] than their complementary bonds [Ti(1)−N(a), Ti(2)−N(d), *d* = 2.147 Å] which suggests that the halves in **1** can be described as bound together by predominantly amido-type bridging bonds rather than donor-acceptor interactions. A similar situation has been found for the bridging amido functions in the complex $[TiN_4C_{12}H_{24}]_2$ ($N_4C_{12}H_{24}$ = tetraamide of 1,5,9,13-tetraazacyclohexadecane)[17] and the alkoxy groups in $[Me_2NTi(OCH_2CH_2)_3N]_2$[3].

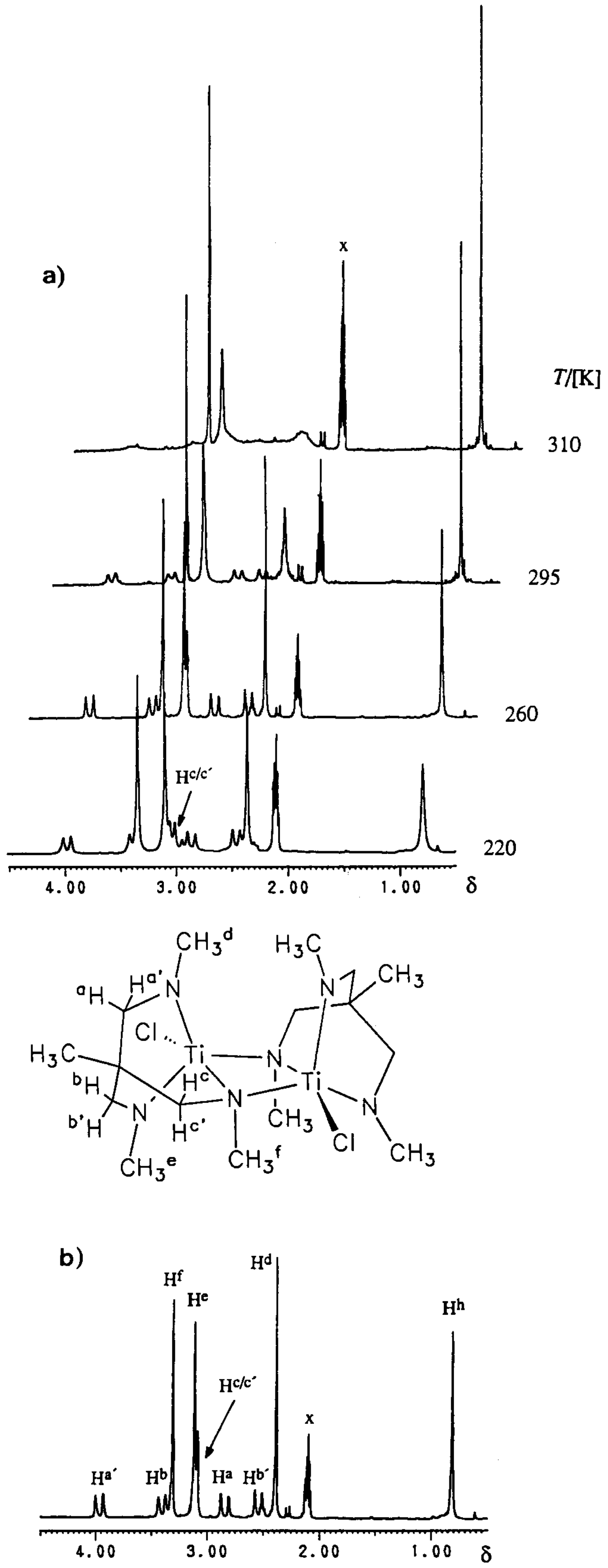

Figure 3. a) Series of variable temperature ^1H-NMR spectra of **1** recorded in [D_8]toluene; b) ^1H-NMR spectrum of **1** recorded at 265 K; the assignment is based on a ^1H-NOESY spectrum as well as selective decoupling experiments (x = solvent)

The structure as shown in Figure 1 might suggest the existence of a second structural isomer in which the two halves of the molecule are related to each other by a centre of inversion at the mid point of the Ti—Ti vector. This, however, would imply a planar Ti_2N_2 ring at the centre of the structure, a situation which would require a considerable distortion of the tripodal chelating amido ligand. We believe that this is the reason for the absence of a signal set attributable to such an isomer in the NMR spectra.

C. The Dynamic Behaviour of 1 in Solution

While the ^1H-NMR spectrum of **1** recorded at 295 K in [D_8]toluene (Figure 3a) represents a more complicated structure than that of **2a**, **b** and **3a**, **b**, the broad resonances observed at this temperature indicate the presence of dynamic processes on the NMR time scale. Lowering the temperature to 260 K effects a marked sharpening of the signals. The assignment of the spectrum displayed in Figure 3b is based on decoupling experiments and a phase-sensitive NOESY spectrum which will be discussed in more detail below. The singlets at δ = 2.43, 3.14, and 3.33 are assigned to the ^1H nuclei of the three *N*-bound methyl groups d, e, and f, respectively. The methylene protons are expected to appear as AB spin systems as is observed for $H^{a/a'}$ (δ = 2.88/4.01, respectively) and $H^{b/b'}$ (δ = 3.44/2.60). The fact that H^c and $H^{c'}$ appear as a slightly broadened singlet resonance indicates residual fluxionality in the molecule. Indeed, if the sample is further cooled to 220 K the resonance splits into the familiar AB pattern.

On heating the solution of **1** to above 295 K, coalescence occurs at 312 K with complete disappearance of all signals except those attributable to the H^e and $H^{c/c'}$ nuclei. Further increase of the temperature above 325 K leads to complex resonance patterns which are complicated by the setting in of thermally induced irreversible transformations of the compound.

In order to establish the exchange network of the dynamic system unambiguously, a phase-sensitive ^1H-NOESY spectrum was recorded at 275 K, i.e. a temperature at which all the signals representing nuclear positions involved in the chemical exchange are slightly broadened. The phase-sensitive NOESY pulse sequence ($\pi/2$-τ-$\pi/2$-t_{mix}-$\pi/2$-FID; τ = time increment of the evolution period, t_{mix} = mixing time)[18] generates off-diagonal cross peaks between nuclei that are coupled through space either by a dipole-dipole (NOE) interaction or by chemical exchange. It should be pointed out that for small or medium-size molecules such as **1** with short correlation times τ_{corr} in solution (fast motion limit: $\tau_{corr} \ll \omega_0^{-1}$), these NOE cross peaks are of opposite phase to that of the diagonal peaks. Cross peaks of the same phase as the diagonal are due to chemical exchange on the time scale of the experiment defined by the mixing time t_{mix}. The latter set of non-diagonal peaks is frequently referred to as the EXSY spectrum.

The NOESY experiment was performed with mixing times of 0.2, 0.5, and 2.0 s. In the spectrum recorded with the shortest mixing time only cross peaks with a phase equal

Scheme 2. NOE and EXSY connections as deduced from a phase-sensitive ^{1}H-NOESY spectrum of **1** recorded at 275 K; the expected NOE cross peak between H^a and H^b could not be observed due to coincidence with a more intense positive phase EXSY cross peak

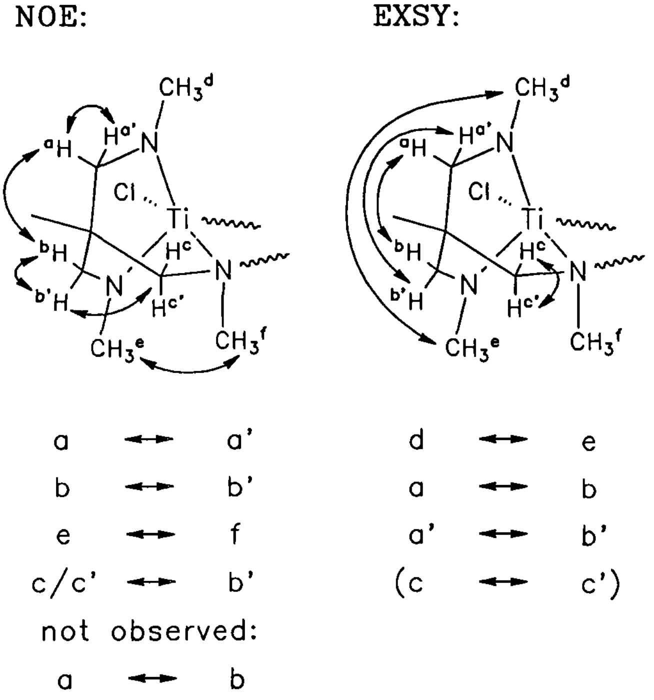

Scheme 3. Overall process effecting the permutation of the different nuclear positions as derived from the ^{1}H-EXSY and variable temperature NMR studies

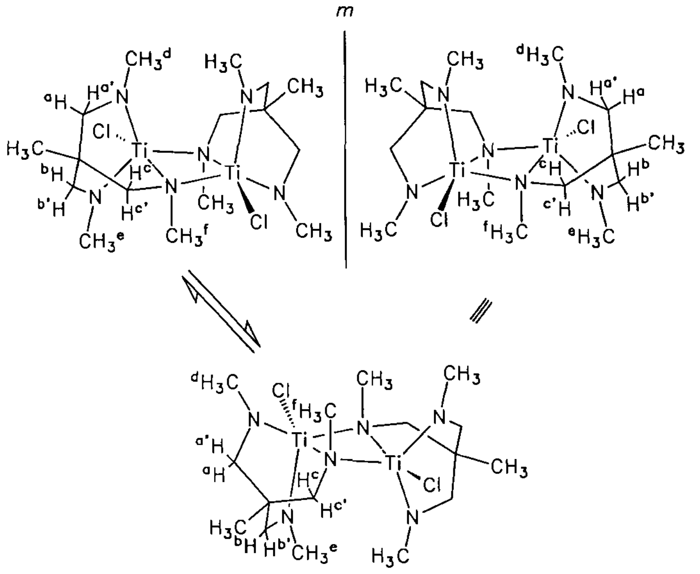

to those along the diagonal were observed, thus representing the EXSY spectrum. Spectral features of the opposite phase barely rose above the noise level. The NOE-related part of the spectrum could be readily observed on increasing the mixing time to 0.5 s, or even more prominently with t_{mix} = 2.0 s (under these conditions the EXSY cross peaks were markedly less intense). In Figure 4 the result of the experiment with t_{mix} = 0.5 s is displayed. For clarity the positive and negative levels of the contour plot are shown separately. The NOE connections established by the negative-phase cross peaks (relative to the diagonal which is shown in a positive absorption mode) are depicted above the diagonal, whereas the exchange network represented by the positive-phase cross peaks is shown below the diagonal.

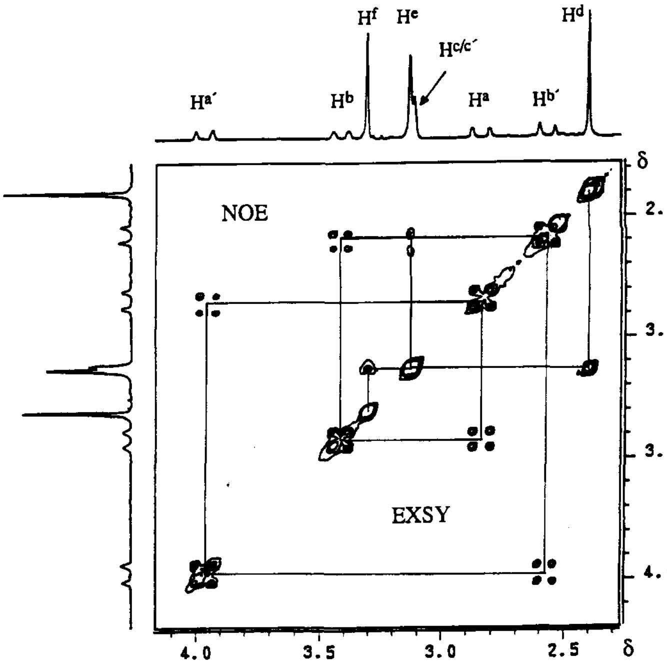

Figure 4. Phase-sensitive ^{1}H-NOESY spectrum of **1** recorded at 275 K. The NOE network (negative levels) is diplayed above, the EXSY network (positive levels) below the diagonal

The NOE and the EXSY networks are summarized in Scheme 2. While the former supports the assignment given in Figure 3b, the latter provides the basis for a mechanistic model of the ligand dynamics. The overall process effecting the permutation of the different nuclear positions is shown in Scheme 3 and represents the interconversion of the two enantiomeric forms of **1**.

To account for such a process, the cleavage of at least two amido-N–Ti bonds within the central Ti_2N_2 unit described in section B must be assumed. In principle, there are two symmetrical ways of opening the Ti_2N_2 ring labelled a and b in Scheme 4. The former involves the two long Ti–N bonds within the ring and leaves the dimer intact, whereas b splits the molecule into two disconnected halves.

Considering the first of the two options, a, the open intermediate thus formed is sufficiently flexible to permit the structural rearrangement required for the interconversion postulated in Scheme 3. Furthermore, the Ti–N bond length pattern established by the crystal structure analysis would also support this pathway. On the other hand, the second alternative, b, may be operative at high temperatures and lead to reaction pathways which are responsible for the irreversible transformations under these conditions.

The overall dynamic model discussed here is additionally supported by the variable temperature series of $^{13}C\{^1H\}$-

Scheme 4. Mechanistic model accounting for the racemisation of 1 on the NMR time scale

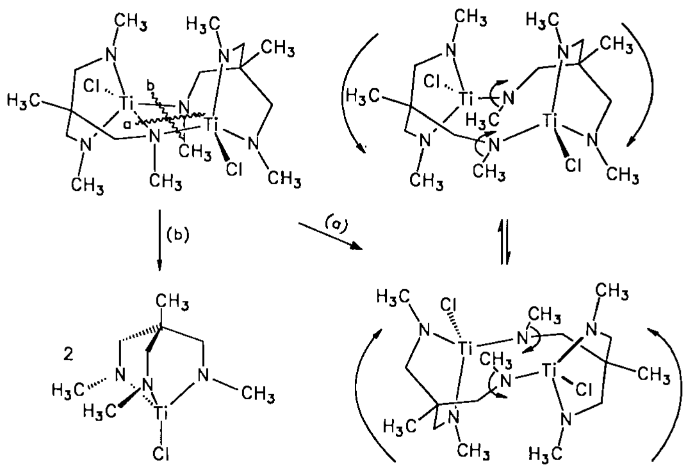

NMR spectra depicted in Figure 5. The three low-field signals at δ = 69.3, 72.1, and 75.8 are the resonances of the *N*-bound methylene groups (C_a, C_b, C_c) in the ligand framework, while the signals at δ = 46.8, 47.4, and 48.4 represent the three *N*-bound methyl groups (C_d, C_e, C_f). The resonances of the quarternary carbon atom (C_g) and the apical CH_3 group (C_h) appear at δ = 43.8 and 24.1 (not shown), respectively. On raising the temperature from 275 to 305 K, the resonances of C_d and C_e coalesce (T_c = 308 K) and reappear as a broad singlet at T = 340 K. At this temperature C_a and C_b have coalesced (exact T_c = 332 K). The spectrum at 365 K represents an effective molecular C_{2h} symmetry of **1** which is consistent with an averaged structure of the two interconverting enantiomers. It should be noted that at the highest temperature additional signals (marked with an asterisk) appear, representing the thermal decomposition products referred to above. The coalescence temperature for the C_a/C_b and C_d/C_e resonances permits the calculation of the free activation enthalpy for the overall exchange process: $\Delta G^{\neq} = 15.4 \pm 0.3$ kcal mol^{-1}.

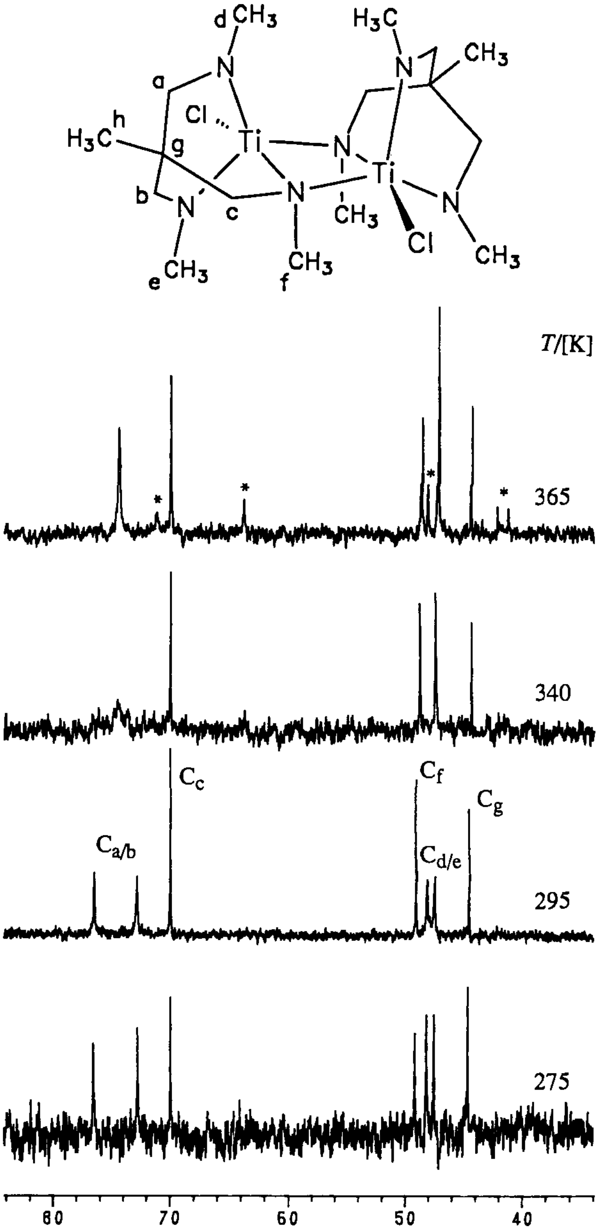

Figure 5. Variable temperature ^{13}C-NMR spectra of **1**; the additional resonances appearing at 365 K which are due to unidentified thermal degradation products are marked with asterisks

D. Isolation of $[H_3CC(CH_2NSiMe_3)_2(H)CH_2NTiX]_2$ (X = Cl **4a**, Br **4b**) and X-ray Crystal Structure Analysis of **4a**

The fact that the tripodal amido complexes **2a**, **b** and **3a**, **b** are only obtained in moderate yields (35–70%) may be partly due to the loss incurred in the workup by distillation. Another reason is the formation of a principal byproduct in their synthesis which in the preparation of **2a** and **2b** crystallises directly from the reaction mixture. Greater amounts of the same material may be isolated by extracting the distillation residue of **2a** and **2b** with pentane and crystallisation of the byproducts **4a** and **4b** from this extract.

$[H_3CC(CH_2NSiMe_3)_2(H)CH_2NTiX]_2$ **4a**: X = Cl
b: X = Br

The analytical data of these solids indicate the loss of one of the trimethylsilyl groups in the original ligand system. The signals assigned to the *N*-bound methylene groups in the ^{1}H- and ^{13}C-NMR spectra of **4a** and **4b** indicate a different local symmetry (C_s) of this part of the molecule in comparison with the C_{3v}-symmetrical amido complexes which are the main products of this reaction. One of the resonances, in particular, has a chemical shift outside the range normally observed for CH_2 groups adjacent to an amido function [**4a**: δ(^{1}H) = 4.65, δ(^{13}C) = 85.8; **4b**: δ(^{1}H) = 4.70, δ(^{13}C) = 86.2]. On the other hand, this shift is characteristic of μ-imido groups[1,19]. The coupling pattern of these methylene protons observed in the ^{1}H-NMR spectra recorded at 295 K supports the above mentioned reduction of the local symmetry from C_{3v} to C_s. The signal at low field appears as a broad singlet while the resonances of the other two chemically equivalent CH_2 groups split into what appears to be an AB pattern [**4a**: $\delta(^1H)$ = 3.51, 3.81; **4b**: 3.48, 3.85] the low-field component of which being somewhat broadened. On raising the temperature to 355 K, the signals sharpen up and display a long-range coupling pattern which is partially resolved. This may be analysed as representing an AA′MM′XX′ spin system in which the protons of the respective methylene groups with relative W geometry show resolved $^4J_{HH}$ coupling. Since the multiplet structure was not fully resolved, the ^4J values could only be roughly estimated by simulation of the spectra to lie within a range of 1.0 – 1.5 Hz.

Whereas the NMR-spectroscopic data are thus consistent with a probably dimeric μ-imido/amido complex, the structural arrangement as well as the complete formulation of the compound remained ambiguous. In order to establish the overall structure, a single crystal X-ray structure analysis of **4a** was carried out. A view of its molecular structure is depicted in Figure 6 along with the principal bond distances and interbond angles.

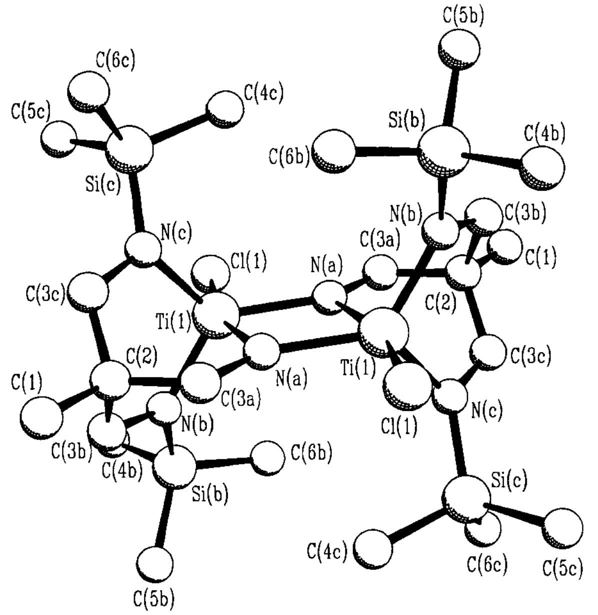

Figure 6. Molecular structure of **4a** in the crystal. Selected bond lenghts [Å] and interbond angles [°]: Ti(1)–Cl(1) 2.313(2), Ti(1)–N(c) 1.866(7), Ti(1)–N(a) 2.030(5), Ti(1)–Ti(1′) 3.225(3), Ti(1)′–N(a) 1.982(5), Si(b)–N(b) 1.731(7), Ti(1)–N(b) 1.876(5), Si(c)–N(c) 1.728(6); N(a)–Ti(1)–Cl(1) 162.1(2), C(3a)–N(a)–Ti(1) 114.1(6), N(b)–Ti(1)–Cl(1) 100.5(2), C(3b)–N(b)–Ti(1) 113.6(6), N(c)–*Ti(1)–Cl(1) 102.1*(2), C(3c)–N(c)–Ti(1) 112.9(5), Si(b)–N(b)–Ti(1) 126.8(4), N(b)–Ti(1)–N(a) 89.7(2), Si(c)–N(c)–Ti(1) 127.2(3), N(c)–Ti(1)–N(a) 89.4(3), Ti(1)–N(a)–Ti(1′) 107.0(2), N(c)–Ti(1)–N(b) 104.1(3), N(a)–Ti(1)–N(a′) 73.0(2)

The centre piece of the dimeric structure is a planar Ti_2N_2 ring [∢ Ti(1)–N(a)–Ti(1)′ = 107.0(2)°; ∢ N(a)–Ti(1)–N(a)′ = 73.0(2)°] arranged around a crystallographic centre of inversion which relates the two halves of the molecule to each other. The non-hydrogen atom framework as shown in Figure 6 has idealised C_{2h} symmetry, the mirror plane being spanned by Ti(1/1′), N(a/a′), C(3a/a′), C(2/2′), C(1/1′) (in the crystal structure this section of the molecule is planar to within 0.011 Å). The bridging N atoms have a planar coordination geometry characteristic of μ-imido ligands. The neopentane framework of the tripodal triamido ligand is preserved and links the imido unit to the remaining two Me_3SiN functions. The coordination of each Ti centre may be viewed as being distorted trigonal-bipyramidal, reminiscent of that found in polymeric $[Me_3SiNTiCl_2]_x$[20], with the two apical positions occupied by one μ-imido N atom and the chlorine atom [∢ N(a)–Ti(1)–Cl(1) = 161.8°] and the equatorial positions by the other imido N atom and the two Me_3SiN functions. The amido-N–Ti bond distances [*d*(Ti–N) = 1.872 Å] are comparable to that found in Roesky's $CpTiCl_2[N(SiMe_3)_2]$[14] but somewhat shorter than those in most other Ti complexes containing chelating silyl amides[12–15].

The bond length pattern within the central Ti_2N_2 ring [*d*{Ti(1)–N(a)} = 1.972, *d*{Ti(1′)–N(a)} = 2.037 Å] classifies this structure as of the asymmetrically bridging imido type. The degree of bond distance alternation lies between the extreme cases reported by Nugent et al. {asymmetric bridging in $[(CH_3)_2(t\text{BuN})W]_2(\mu\text{-}t\text{BuN})_2$: *d*(W–N) = 1.842(4) and 2.288(5) Å; symmetric bridging in $[((CH_3)_2N)_2Ti]_2(\mu\text{-}t\text{BuN})_2$: *d*(Ti–N) = 1.921(2) and 1.925(2) Å}[21–23]. The asymmetry of the imido-bridged tungsten compound was interpreted by the authors as a consequence of a second-order Jahn-Teller distortion around the five-coordinate metal centres and thought to reflect a different π- and σ-bonding topology in comparison with their symmetrical Ti compound. While **4a** has a coordination geometry at the Ti atoms which is related to that of Nugent's W_2N_2 structure, the presence of the chelating ligand system in **4a** and the resulting geometrical constraints due to this situation make a case along the same lines of argument less convincing.

The structure as shown here is incomplete as far as the nature of the nitrogen ligands involved is concerned. Since **4a** is a neutral Ti(IV) compound, two of the N atoms in the dimer must be protonated in order to give a meaningful stoichiometric formula. However, a careful scrutiny of the crystal structure gave no indication as to the location of these protons. This may be a consequence of either a static or dynamic disorder of these H atoms between the N centres. Since the thermal parameters of the atoms involved show no anomaly attributable to significant disorder within the non-hydrogen framework [N(a) is slightly more ellipsoidal that the other N atoms], the effect that N protonation has on the geometry of the ligand must be rather small. All N atoms are planar coordinated as is expected for amido and imido functions, and all Ti–N distances lie within the expected range, so that even an indirect determination of these additional H positions is precluded. This is in contrast to the structure of $[O(TiN_4C_{12}H_{25})_2]$ ($N_4C_{12}H_{25}$ = the monoprotonated tetraamide of 1,5,9,13-tetraazacyclohexadecane) which contains a protonated polydentate amido ligand, and in the X-ray structure analysis of which a direct location of the N–H hydrogen atoms was possible[17].

That **4a** (and similarly **4b**) is indeed a protonated amide can be inferred from its spectroscopic properties. A weak band in the IR spectrum of the compound at 3172 cm^{-1}

(**4b**: 3160 cm^{-1}) may be attributed to a $\nu(N-H)$ mode. Additional evidence originates from the indirect effect the highly dynamic protons have on the ^1H-NMR spectrum of the compound. At 295 K weak and on cooling to 180 K significant broadening of all methylene ^1H resonances is observed. Coalescence occurs below 180 K, and it was thus not possible to freeze out the dynamic process. Neither the location of the exchanging protons nor a mechanistic model for their exchange could therefore be deduced. Despite numerous attemps, we have not succeded in directly observing these $N-H$ nuclei within a chemical shift range of $\delta = 0.0-15.0$.

As to the formation of **4a** and **4b**, it should be pointed out that both compounds do not appear to be thermal degradation products of **2a** and **2b**. The latter may be distilled in vacuo without decomposition. Both species are clearly generated as byproducts in the substitutions leading to the amido complexes. Since great care was taken to avoid the presence of moisture in the solvents used in the synthesis as well as in the course of the workup of **2a** and **2b**, and in view of the amounts of **4a**, **b** isolated, a conceivable hydrolytic desilylation may be disregarded. We therefore propose that the N–H protons in **4a**, **b** originate from the solvents present in the reaction mixture [probably THF from $TiX_4(THF)_2$] which are activated by unsaturated Ti-imide intermediates generated by dechloro/bromosilylation of the partially coordinated amido tripod. This would be reminiscent of a similar C–H activation processes reported by Wolczanski et al. for unsaturated Ti=N and Zr=N species[16,24]. Since the complicated nature of the formation of **2a**, **b** from their precursors and the accompanying degradation processes have prohibited the spectroscopic monitoring of this reaction, the explanation offered here could thus far not be substantiated.

Conclusion

The aim of this study was the synthesis of a new class of mixed amido-halide Ti complexes using a tripodal ligand system developed previously by us. This may constitute an alternative to the known azatitanatranes which have recently found considerable attention. In spite of the unsatisfactory yields in which some of these compounds are obtained, a series of thermally stable Ti complexes with one remaining reactive site is now available in gram quantities.

Investigations into the reactivity of these compounds as well as their potential use as building blocks in the generation of oligonuclear structures are underway. We are also currently extending the use of the tripodal amido ligands to the metals of the V and Cr triads.

We would like to thank Prof. *H. Werner* for support of this work and the *Fonds der Chemischen Industrie* for a research fellowship (to L. H. G.). M. McP. and A. J. E. acknowledge financial support by the *SERC*.

Experimental

All experiments were carried out under dry Ar by using standard (Schlenk) glassware which was flame-dried prior to use. The solvents were dried over Na or Na/K alloy, distilled and saturated with argon. The deuterated solvents used for the NMR-spectroscopic measurements were dried over 4-Å molecular sieves.

^1H-, ^{13}C- and ^{29}Si-NMR: Bruker AC 200 (at 200.13, 50.32, and 39.76 MHz, respectively), B-VT-2000 variable temperature unit. – ^1H-EXSY spectra (recorded at 275 K): Bruker automation programmes NOESY (absolute magnitude mode) and NOESPHPC (phasesensitive TPPI mode). 128 1K-FID's of 16 scans over a sweep width of 844 Hz were collected; the mixing time was set at 0.2, 0.5 and 2.0 s which was randomly varied within a range of ±25 ms to suppress *J*-cross peaks (confirmed by a ^1H-COSY spectrum). The F1 dimension was zero-filled to 512W and 1K (phase-sensitive mode) prior to Fourier transformation, apodization (π/3-shifted sine bell) and phase correction. All the 2D spectra were symmetrized. – IR: Bruker IRS 25 FT. – Elemental analyses: Microanalytical laboratory of the Chemistry Dept. at Würzburg. – $H_3C(CH_2NHCH_3)_3$, $H_3C(CH_2NHSiMe_3)_3$, and $H_3C(CH_2NH[tBuSiMe_2])_3$ were prepared as reported previously by us[7]. $TiCl_4(THF)_2$ and $TiBr_4(THF)_2$ were prepared according to literature procedures[25]. All other chemicals used as starting materials were obtained commercially and used without further purification.

1) *1,1,1-Tris{[(tert-butyldimethylsilyl)amino]methyl}ethane:* B.p. 123 °C/0.1 Torr. – ^1H NMR ($CDCl_3$, 295 K): $\delta = -0.05$ [s, $Si(CH_3)_2$], 0.66 (s, CH_3C), 0.85 [s, $C(CH_3)_3$], 2.53 [d, CH_2NH, $^3J_{HH(N)} = 8.0$ Hz]. – $^{13}C\{^1H\}$ NMR ($CDCl_3$, 295 K): $\delta = -5.1$ [$Si(CH_3)_2$], 18.5 [$SiC(CH_3)_3$], 26.1 (CH_3-C), 26.5 [$SiC(CH_3)_3$], 40.7 (CH_3-C), 48.4 (CH_2N). – $^{29}Si\{^1H\}$ NMR ($CDCl_3$, 295 K): $\delta = 8.1$. – IR (neat): $\tilde{\nu} = 3385$ cm^{-1} m, 2940 s, 2920 s, 2880 s, 2840 s, 1660 w br, 1460 s, 1395 s, 1383 s, 1355 m, 1250 vs, 1130 s, 1090 s br, 1002 s, 825 vs br, 774 s, 640 m. – $C_{23}H_{57}N_3Si_3$ (460.0): calcd. C 60.06, H 12.49, N 9.14; found C 60.46, H 12.81, N 9.38.

2) *$[H_3CC(CH_2NCH_3)_3TiCl]_2$* (**1**): To a stirred solution of 2.53 g (15.88 mmol) of $H_3CC(CH_2NHCH_3)_3$ in 90 ml of pentane/diethyl ether (2:1), which was cooled to –40 °C, was slowly added 50.0 mmol of *n*BuLi (20.0 ml of a 2.5 M solution in hexane). The reaction mixture was warmed to room temp. and, after the butane evolution had subsided, heated under reflux for a short period of time. After the solution of the lithiated amine had been stirred at room temp. for another 30 min, it was cooled to –50 °C, then 5.94 g (17.80 mmol) of solid $TiCl_4(THF)_2$ was added. The reaction mixture was warmed to room temp. over a period of 15 h and the solvent evaporated in vacuo. The residue was extracted with toluene, the extract filtered and the volume of the solution reduced to ca. 5 ml. Storage at –60 °C yielded **1** as a red crystalline solid. Isolated yield: 0.74 g (19%). – ^1H NMR ([D_8]toluene, 295 K): $\delta = 0.85$ (s, CH_3C), 2.43 (s, ^dH_3CN), 2.60 (d, $^{b'}H_2CN$, $^2J_{^bH^{b'}H} = 12.7$ Hz), 2.88 (d, ^aH_2CN, $^2J_{^aH^{a'}H} = 13.9$ Hz), 3.12 (s, $^{c/c'}H_2CN$), 3.14 (s, ^eH_3CN), 3.31 (s, ^fH_3CN), 3.44 (d, ^bH_2CN), 4.01 (d, $^{a'}H_2CN$). – $^{13}C\{^1H\}$ NMR (C_6D_6, 295 K): $\delta = 24.1$ (CH_3-C), 43.8 (CH_3-C), 46.8, 47.4, 48.3 (CH_3N), 69.3, 72.1, 75.8 (CH_2N). – IR (toluene): $\tilde{\nu} = 2940$ cm^{-1} m, 2924 m, 2864 w, 2840 w, 1604 s, 1496 vs, 1456 m, 1260 s, 1084 s, 1068 m, 1032 s, 1016 m, 808 s, 736 vs. – $C_{16}H_{36}Cl_2N_6Ti_2$ (479.2): calcd. C 40.10, H 7.57, N 17.54; found C 40.07, H 7.63, N 17.28.

3) *Synthesis of $H_3CC(CH_2NSiMe_2R)_3TiX$ (R = Me, X = Cl:* **2a**; *R = Me, X = Br:* **2b**: *R = tBu, X = Cl:* **3a**; *R = tBu, X = Br:* **3b***) and Isolation and Characterisation of $[H_3CC(CH_2NSiMe_3)_2(H)CH_2NTiX]_2$ (X = Cl:* **4a**, *X = Br:* **4b***):* To a stirred solution of 7.61 mmol of $H_3CC(CH_2NHSiMe_2R)_3$ (R = Me, *t*Bu) in 60 ml of pentane, which was cooled to –50 °C, 22.75 mmol of *n*BuLi (9.1 ml of a 2.5 M solution in hexane) was slowly added. The reaction mixture was warmed to room temp. and subsequently heated under reflux for 1 h. During this time the amide precipitated

as a colourless solid. After cooling to room temp. and subsequent stirring for another 30 min, the suspension was cooled to $-50\,^{\circ}C$ and 8.50 mmol of solid $TiX_4(THF)_2$ (X = Cl, Br) was added. The reaction mixture was warmed to room temp. over a period of 15 h, filtered through a G3 frit and the solvent of the filtrate removed in vacuo. Vacuum distillation of the residue yielded **2a**, **2b**, **3a**, and **3b** as bright orange oils [Yields: **2a** 1.54 g (49%), **2b** 2.34 g (67%), **3a** 1.69 g (41%), **3b** 1.60 g (36%)]. The residues in the distillation flasks of **2a** and **2b** were taken up in pentane, and the solutions were cooled to 5 °C. After 2–4 d yellow crystalline **4a** or orange brown microcrystalline **4b** were isolated and purified by washing with cold pentane. Yields **4a** 313 mg (12%), **4b** 107 mg (4%).

2a: B.p. 116 °C/0.2 Torr. – ^1H NMR (C_6D_6, 295 K): $\delta = 0.19$ [s, $Si(CH_3)_3$], 0.89 (s, CH_3C), 3.45 (s, CH_2N). – $^{13}C\{^1H\}$ NMR (C_6D_6, 295 K): $\delta = 0.9$ [$Si(CH_3)_3$], 25.4 (CH_3-C), 50.0 (CH_3-C), 62.6 (CH_2N). – $^{29}Si\{^1H\}$ NMR (C_6D_6, 295 K): $\delta = 0.3$. – IR (neat): $\tilde{\nu} = 2956\ cm^{-1}$ m, 2896 w, 2868 w, 2824 w, 1248 s, 1132 w, 1048 m, 992 w, 920 s, 836 vs, 756 w, 684 w. – $C_{14}H_{36}ClN_3Si_3Ti$ (414.1): calcd. C 40.61, H 8.76, N 10.15; found C 40.99, H 9.12, N 10.02.

2b: B.p. 111 °C/0.1 Torr. – ^1H NMR (C_6D_6, 295 K): $\delta = 0.23$ [s, $Si(CH_3)_3$], 0.87 (s, CH_3C), 3.42 (s, CH_2N). – $^{13}C\{^1H\}$ NMR (C_6D_6, 295 K): $\delta = 1.3$ [$Si(CH_3)_3$], 25.4 (CH_3-C), 50.5 (CH_3-C), 62.7 (CH_2N). – $^{29}Si\{^1H\}$ NMR (C_6D_6, 295 K): $\delta = 0.2$. – IR (neat): $\tilde{\nu} = 2956\ cm^{-1}$ m, 2896 vw, 2868 vw, 2824 w, 1248 s, 1132 vw, 1036 w, 992 w, 920 s, 832 vs, 756 m, 684 vw. – $C_{14}H_{36}BrN_3Si_3Ti$ (458.5): calcd. C 36.67, H 7.91, N 9.16; found C 37.76, H 7.75, N 9.01.

3a: B.p. 163 °C/0.02 Torr. – ^1H NMR (C_6D_6, 295 K): $\delta = 0.27$ [s, $Si(CH_3)_2$], 0.92 (s, CH_3C), 0.96 [s, $C(CH_3)_3$], 3.57 (s, CH_2N). – $^{13}C\{^1H\}$ NMR (C_6D_6, 295 K): $\delta = -3.0$ [$Si(CH_3)_2tBu$], 20.1 [$Si(C(CH_3)_3)Me_2$], 25.4 (CH_3-C), 27.2 [$Si(C(CH_3)_3)Me_2$], 51.8 (CH_3-C), 63.7 (CH_2N). – $^{29}Si\{^1H\}$ NMR (C_6D_6, 295 K): $\delta = 5.5$. – IR (neat): $\tilde{\nu} = 2956\ cm^{-1}$ vs, 2928 s, 2884 m, 2856 s, 1468 m, 1388 w, 1252 s, 1092 w, 1040 m, 992 w, 916 m, 828 vs, 768 s, 736 w, 672 w,. – $C_{23}H_{54}ClN_3Si_3Ti$ (540.3): calcd. C 51.13, H 10.07, N 7.78; found C 52.36, H 10.29, N 8.01.

3b: B.p. 174 °C/0.05 Torr. – ^1H NMR (C_6D_6, 295 K): $\delta = 0.30$ [s, $Si(CH_3)_2tBu$], 0.89 (s, CH_3C), 0.96 [s, $C(CH_3)_3$], 3.54 (s, CH_2N). – $^{13}C\{^1H\}$ NMR (C_6D_6, 295 K): $\delta = -2.4$ [$Si(CH_3)_2tBu$], 20.2 [$Si(C(CH_3)_3)Me_2$], 25.5 (CH_3-C), 27.3 [$Si(C(CH_3)_3)Me_2$], 52.5 (CH_3-C), 63.8 (CH_2N). – $^{29}Si\{^1H\}$ NMR (C_6D_6, 295 K): $\delta = 5.5$. – IR (neat): $\tilde{\nu} = 2952\ cm^{-1}$ vs, 2928 s, 2884 m, 2856 s, 1468 m, 1404 w, 1388 w, 1252 s, 1132 w, 1096 w, 1036 w, 1008 vw, 992 vw, 920 m, 828 vs, 768 s, 664 w. – $C_{23}H_{54}BrN_3Si_3Ti$ (584.7): calcd. C 47.24, H 9.31, N 7.19; found C 47.56, H 9.40, N 7.53.

4a: ^1H NMR ([D_8]toluene, 295 K): $\delta = 0.50$ [s, $Si(CH_3)_3$], 0.89 (s, CH_3C), 3.71 (d, $CHH-NSi$, $^2J_{HH} = 12.3$ Hz), 4.01 (d, $CHH-NSi$), 4.85 (s, CH_2NTi). – $^{13}C\{^1H\}$ NMR ([D_8]toluene, 295 K): $\delta = 1.4$ [$Si(CH_3)_3$], 21.9 (CH_3-C), 50.2 (CH_3-C), 65.9 (CH_2NSi), 85.8 (CH_2NTi). – $^{29}Si\{^1H\}$ NMR ([D_8]toluene, 295 K): $\delta = 10.1$. – IR (*n*-hexane): $\tilde{\nu} = 3172\ cm^{-1}$ vw, 2948 vs, 2916 vs, 2884 vs, 2852 vs, 1460 vs, 1380 s, 1248 m, 1140 w, 1052 w, 988 w, 952 w, 928 vw, 852 s, 756 w. – $C_{22}H_{56}Cl_2N_6Si_6Ti_2$ (683.8): calcd. C 38.65, H 8.26, N 12.29; found C 37.98, H 8.01, N 12.44.

4b: ^1H NMR (C_6D_6, 295 K): $\delta = 0.34$ [s, $Si(CH_3)_3$], 0.59 (s, CH_3C), 3.48 (d, $CHH-NSi$, $^2J_{HH} = 12.2$ Hz), 3.85 (d, $CHH-NSi$), 4.70 (s, CH_2NTi). – $^{13}C\{^1H\}$ NMR (C_6D_6, 295 K): $\delta = 0.8$ [$Si(CH_3)_3$], 21.2 (CH_3-C) 49.2 (CH_3-C), 65.2 (CH_2NSi), 86.2 (CH_2NTi). – $^{29}Si\{^1H\}$ NMR (C_6D_6, 295 K): $\delta = 5.3$. – IR (*n*-hexane): $\tilde{\nu} = 3160\ cm^{-1}$ w, 2964 vs, 2932 vs, 2900 vs, 2868 s, 1456 vs, 1380 s, 1260 m, 1136 w, 1100 m, 1064 w, 1036 w, 984 w, 952 vw, 928 vw, 852 s, 808 w, 776 vw. – $C_{22}H_{56}Br_2N_6Si_6Ti_2$ (772.6): calcd. C 34.20, H 7.31, N 10.88; found C 34.04, H 7.11, N 10.82.

4) *X-ray Crystallographic Study of* **1** *and* **4a**: The clear, red crystals of **1** as well as the yellow crystals of **4a** had a prismatic habit. A regularly shaped crystal of **1** with the approximate dimensions of 0.32 × 0.26 × 0.20 mm was mounted under argon in a Lindemann capillary; a regular, block-shaped crystal of **4a** with the approximate dimensions 0.48 × 0.40 × 0.40 mm was mounted in a similar way. The X-ray diffraction data were collected by using a Philips PW 1100 diffractometer with graphite-monochromated Mo-K_{α} radiation. Unit cell parameters were determined by a least-squares analysis of 25 automatically centred reflections in the range of 10° $< \Theta <$ 15°. Data were collected at 295 K in the range of Θ = 3–25° with a scan width of 0.80° by using the technique described previously[26]. Details are presented in Table 1.

The data analysis and refinement were carried out with the programmes of the SHELX 76 software package[27]. The coordinates of the titanium atoms were deduced from a Patterson synthesis. The remaining non-hydrogen atoms were located from subsequent difference Fourier syntheses and refined with anisotropic thermal parameters assigned to all non-hydrogen atoms. The positions of the C-bound hydrogen atoms in both structures were located in electron density difference maps and were included in the structure

Table 1. Crystal data and experimental details for **1** and **4a**

	1	**4a**
Empirical formula	$C_{16}H_{36}Cl_2N_6Ti_2$	$C_{22}H_{56}Cl_2N_6Si_6Ti_2$
Formula weight	479.28	683.78
Crystal system	monoclinic	monoclinic
a [Å]	11.961(2)	11.634(2)
b [Å]	22.627(4)	14.899(3)
c [Å]	8.403(2)	12.110(2)
β [°]	97.88(2)	116.12(2)
V [Å^3]	1053.2	1884.71
Z	4	4
$D_{calcd.}$ [gcm^{-1}]	1.41	1.20
Space group	$P2_1/n$	$P2_1/c$
*F*000	1008	724
μ(Mo K_{α}) [cm^{-1}][a]	9.3	6.9
θ range [°]	3 - 25	3 - 25
No. of observed reflexions $I > 3.00\ \sigma(I)$[b]	1362	1876
No. of variables[c]	157	110
Residuals: *R*; R_w	0.0653; 0.0593	0.0650; 0.0705
Data/parameter	8.6	16.8
Largest peak/hole in final difference map [e$^-$A^{-3}]	+0.45/-0.44	+0.60/-0.42

[a] An empirical absorption correction, using the programme DIFABS (N. Walker; D. Struart, *Acta. Crystallogr., Sect. A*, **1983**, *39*, 158) was applied for both crystals: the data were corrected for Lorentz and polarization effects. – [b] The intensities of three representative reflections were measured every 5 h of X-ray exposure time; they remained constant throughout the data collection indicating in both cases crystal and electronic stability (no decay correction was applied). – [c] Neutral atom scattering factors were taken from D. T. Cromer, J. T. Waber, *International Tables of X-ray Crystallography*, The Kynoch Press, Birmingham, **1974**.

factor calculations with thermal factors of 0.08 Å^2, but their parameters not refined. A careful scrutiny of the structure of **4a** gave no indication of the location of the N-bound H atoms postulated in our formulation of the compound[28].

---

[1] M. H. Chisholm, I. P. Rothwell in *Comprehensive Coordination Chemistry*, vol. 2 (Eds.: G. Wilkinson, R. D. Gillard, J. A. McCleverty), Pergamon, Oxford, **1987**, p. 161.

[2] W. M. P. B. Menge, J. G. Verkade, *Inorg. Chem.* **1991**, *30*, 4628.

[3] A. A. Naiini, W. M. P. B. Menge, J. G. Verkade, *Inorg. Chem.* **1991**, *30*, 5009.

[4] W. Plass, J. G. Verkade, *J. Am. Chem. Soc.* **1992**, *114*, 2275.

[5] C. C. Cummins, R. R. Schrock, W. M. Davis, *Organomet.* **1992**, *11*, 1452.

[6] C. C. Cummins, J. Lee, R. R. Schrock, W. M. Davis, *Angew. Chem.* **1992**, *104*, 1510; *Angew. Chem. Int. Ed. Engl.* **1992**, *31*, 1501.

[7] L. H. Gade, N. Mahr, *J. Chem. Soc., Dalton Trans.* **1993**, 489.

[8] L. H. Gade, C. Becker, J. W. Lauher, *Inorg. Chem.* **1993**, *32*, 2308.

[9] Y. Bai, M. Noltemeyer, H. W. Roesky, *Z. Naturforsch., Teil B*, **1991**, *46*, 1357.

[10] D. G. Dick, R. Rousseau, D. W. Stephan, *Can. J. Chem.* **1991**, *69*, 357.

[11] R. A. Jones, J. G. Hefner, T. C. Wright, *Polyhedron* **1984**, *3*, 1121.

[12] M. H. Chisholm, M. W. Extine, *J. Am. Chem. Soc.* **1977**, *99*, 792.

[13] D. J. Brauer, H. Bürger, K. Wiegel, *J. Organomet. Chem.* **1978**, *150*, 215; H. Bürger, K. Wiegel, U. Thewalt, D. Schomburg, *ibid.* **1975**, *87*, 301; D. J. Brauer, H. Bürger, E. Essig, W. Gschwandtner, *ibid.* **1980**, *190*, 343; W. D. Beiersdorf, D. J. Brauer, H. Bürger, *Z. Anorg. Allg. Chem.* **1981**, *475*, 56.

[14] C. Airoldi, D. C. Bradley, H. Chudzynska, M. B. Hursthouse, K. M. A. Malik, P. R. Raithby, *J. Chem. Soc., Dalton Trans.* **1980**, 2010; D. C. Bradley, H. Chudzynska, J. D. J. Backer-Dirks, M. B. Hursthouse, A. A. Ibrahim, M. Motevalli, A. C. Sullivan, *Polyhedron* **1990**, *9*, 1423. Exceptions are $CpTiCl_2[N(SiMe_3)_2]$ which has a Ti–N bond distance of 1.879(3) Å: Y. Bai, H. W. Roesky, M. Noltemeyer, *Z. Anorg. Allg. Chem.* **1991**, *595*, 21, and $[(t\text{BuNMe}_2\text{Si}t\text{BuN})\text{TiCl}_2]$: R. A. Jones, M. H. Seeberger, J. T. Atwood, W. E. Hunter, *J. Organomet. Chem.* **1983**, *247*, 1.

[15] W. A. Herrmann, M. Denk, R. W. Albach, J. Behm, E. Herdtweck, *Chem. Ber.* **1991**, *124*, 683.

[16] C. C. Cummins, C. P. Schaller, G. D. Van Duyne, P. T. Wolczanski, A. W. E. Chan, R. Hoffmann, *J. Am. Chem. Soc.* **1991**, *113*, 2985.

[17] M. M. Olmstead, P. P. Power, M. Viggiano, *J. Am. Chem. Soc.* **1983**, *105*, 2927.

[18] R. R. Ernst, G. Bodenhausen, A. Wokaun: *Principles of Nuclear Magnetic Resonance in One and Two Dimensions*, Clarendon Press, Oxford, **1987**, p. 490.

[19] R. J. Doedens, *Inorg. Chem.* **1969**, *8*, 570.

[20] N. W. Alcock, M. Pierce-Butler, G. R. Willey, *J. Chem. Soc., Dalton Trans.* **1976**, 707.

[21] D. L. Thorn, W. A. Nugent, R. L. Harlow, *J. Am. Chem. Soc.* **1981**, *103*, 357.

[22] Symmetrically μ-N-bridged imidotitanium complexes have also been reported by Y. Bai, H. W. Roesky, H. G. Schmidt, M. Noltemeyer, *Z. Naturforsch., Teil B* **1992**, *47*, 603.

[23] For other μ-imido complexes, see e.g. S. Gambarotta, C. Floriani, A. Chiesi-Villa, C. Guastini, *J. Am. Chem. Soc.* **1983**, *105*, 7295; C. T. Vroegop, J. H. Teuben, F. van Bolhuis, J. G. M. van der Linden, *J. Chem. Soc., Chem. Commun.* **1983**, 550; J. N. Armor, *Inorg. Chem.* **1978**, *17*, 203; A. A. Danopoulos, G. Wilkinson, B. Hussain-Bates, M. B. Hursthouse, *J. Chem. Soc., Dalton Trans.* **1991**, 269.

[24] C. C. Cummins, C. P. Schaller, P. T. Wolczanski, unpublished results cited in ref.[16]

[25] L. E. Manzer, *Inorg. Synth.* **1982**, *21*, 135.

[26] M. K. Cooper, P. J. Guerney, M. McPartlin, *J. Chem. Soc., Dalton Trans.* **1982**, 757.

[27] G. M. Sheldrick, *SHELX 76, Program for Crystal Structure Determination*, University of Cambridge, **1976**.

[28] Further details of the crystal structure investigations are available on request from the Fachinformationszentrum Karlsruhe, Gesellschaft für wissenschaftlich-technische Information mbH, D-76344 Eggenstein-Leopoldshafen, on quoting the depository number CSD-57441, the names of authors, and the journal citation.

[118/93]